

# Chapter 4

## Study of Blast Wave Problem in a Non-ideal Dusty Gas

### 4.1 Introduction

The study of the effect of solid particles in a dusty gas which is mixture of gas and solid particles, on the growth and decay process of strong shock wave yields interesting results applicable to problems arising in the area of astrophysical fluid. In cases when velocity of mixture is very high, the dust particles presented in the mixture behaves like a pseudo fluid. When a strong shock wave is propagated in a non-ideal gas with dust particles, the radius of strong shock wave, the pressure, the density, the speed of shock wave and the energy carried by a strong shock wave change across the shock, and have a significant difference from those which arise when the strong shock wave passes through an ideal and dust-free gas. A variety of phenomenon occurs in astrophysical fluid where mass fraction of solid particles is very small in comparison to the gas particles such as supernova explosions, photo

ionized gas, volcanic jets, solid particle motion in rocket exhaust etc. Also, a valid guess regarding the propagation of strong shock waves in a non-ideal dusty gas is very important for the design of warfare and operation of space vehicles.

When a large amount of energy is instantaneously released from a core, a disturbance in the medium is propagated headed by a compressive wave, called a blast wave. Such type of problem is formulated mathematically as a system of quasilinear hyperbolic system of partial differential equations. To find the exact solution of the system of equations governing the blast wave problem is almost impossible. In past many attempts have been made to find the analytical/approximate analytical solution of governing system of the blast wave problem using physically relevant assumptions. Taylor (1950a, 1950b) estimated the relationship between the energy input of an extremely powerful explosion and the growth of the resulting fireball and a detailed analysis of Taylor's work is presented by Sedov (1959). Singh et al. (1984) studied the flow behind an attached shock wave in a radiating gas. Sachdev et al. (2005) obtained the exact solutions of compressible flow equations in spherically symmetric coordinate system for ordinary gas. Murata (2006) have derived the exact solution for the one dimensional blast wave problem for ideal gas dynamics with generalized geometry. Singh et al. (2011) studied the imploding shocks in non-ideal magnetogas dynamics using similarity method. Singh et al. (2012) studied the evolution and decay of acceleration waves in radiative magnetogas dynamics Singh et al. (2012) obtained the quasi-similar solution of the strong shock wave problem in non-ideal gas

Due to various important applications of blast wave theory, a continuous improvement in the field is desirable. Since blast wave carries gas and small dust particles, so the study of blast wave problem for non-ideal dusty gas is more realistic than the ordinary gas dynamic system. In the present chapter, an attempt has been made to

find the closed form solution of the system of equations governing the propagation of a blast wave in non-ideal dusty gas with generalized geometry. Here, it is assumed that the density ahead of the shock front varies according to power of the distance from the source of explosion. An expression for the total energy is also determined.

## 4.2 Basic Equations

The governing equations describing a non planar adiabatic non-ideal dusty gas flow are given as (Pai, Memon and Fan 1980 and Chadha and Jena 2014)

$$\frac{\partial \rho}{\partial t} + u \frac{\partial \rho}{\partial x} + \rho \left( \frac{\partial u}{\partial x} + \frac{m}{x} u \right) = 0, \quad (4.2.1)$$

$$\frac{\partial u}{\partial t} + u \frac{\partial u}{\partial x} + \frac{1}{\rho} \frac{\partial p}{\partial x} = 0, \quad (4.2.2)$$

$$\frac{\partial p}{\partial t} + u \frac{\partial p}{\partial x} + c^2 \rho \left( \frac{\partial u}{\partial x} + \frac{m}{x} u \right) = 0, \quad (4.2.3)$$

where  $\rho$ ,  $u$  and  $p$  are density, flow velocity and pressure of the non-ideal dusty gas respectively and  $t > 0$ ,  $x \in R$ .  $c = (((\Gamma - \alpha_2 \rho^2) p) / ((1 - \alpha_1 \rho + \alpha_2 \rho^2)))^{1/2}$  denotes the speed of sound in the non-ideal dusty gas with  $\alpha_1 = \theta + \bar{b}$ ,  $\alpha_2 = \theta \bar{b}$ ,  $\bar{b} = b(1 - k_p)$  where  $b$  is the van der Waals excluded volume and  $k_p = m_{sp}/m_{gd}$  is the mass fraction of solid particles in non-ideal dusty gas, where  $m_{sp}$  and  $m_{gd}$  are the masses of solid particles and non-ideal dusty gas respectively.  $m = 0, 1$  and  $2$  corresponds to the planar, cylindrically symmetric and spherically symmetric flows respectively. The specific heat of non-ideal dusty gas at constant pressure is given by  $c_{pd} = k_p c_{sp} + (1 - k_p) c_p$ , where  $c_p$  and  $c_{sp}$  stands for specific heat of gas and solid particle respectively. If  $c_{vd}$  denotes the specific heat of non-ideal dusty gas at constant volume, the ratio of specific heats for dusty gas is given by Pai (1977) as

$\Gamma = \frac{c_{pd}}{c_{\nu d}} = \frac{\gamma(1+\delta\beta)}{1+\delta\beta}$ , where  $\delta = k_p/(1 - k_p)$ ,  $\beta = c_{sp}/c_p$ ,  $\gamma = c_p/c_\nu$ , with  $c_\nu$  as specific heat of gas at constant volume. Equation of state for adiabatic non-ideal dusty gas flow is given by Chadha and Jena (2014),  $p = \frac{(1-k_p)}{(1-Z)(1-\bar{b}\rho)}\rho\mathcal{R}T$ , where  $Z = (Z_0\rho/\rho_0)$  denotes the volume fraction of small solid particle in the mixture and the subscript “0” denotes the value of physical entities in undisturbed region. The relation between entities  $Z$  and  $k_p$  is given by Pai et al. (1980) as  $k_p = (Z\rho_{sp}/\rho)$ , where  $\rho_{sp}$  stands for density of solid particles in the mixture. Since mass fraction of solid particle must be constant in the equilibrium flow therefore  $\frac{Z}{\rho} = \text{constant}$  (say  $\theta$ ). The relation between  $Z$  and  $k_p$  is also given by  $Z = \frac{k_p}{(1-k_p)\Omega+k_p}$ , where  $\Omega = \rho_{sp}/\rho_g$  is the density fraction of the solid particles.

### 4.3 Boundary Conditions

Let  $R$  be the position of the shock front from the centre of explosion and is a function of time  $t$ , then the propagation velocity of shock front,  $s$ , is given by

$$s = \frac{dR}{dt}. \quad (4.3.1)$$

If ahead of shock front the undisturbed volume fraction of solid particles and density of the mixture are  $Z_0$ ,  $\rho_0$  and pressure, density, velocity just behind the shock are  $p$ ,  $\rho$ ,  $u$ . Then we have the following Rankine-Hugoniot conditions across the shock front (Chadha and Jena (2014))

$$\rho = \frac{\Gamma + 1}{\Gamma - 1 + 2\bar{b}\rho_0 + 2Z_0}\rho_0, \quad (4.3.2)$$

$$u = \frac{2(1 - \bar{b}\rho_0 - Z_0)}{\Gamma + 1}s, \quad (4.3.3)$$

$$p = \frac{2(1 - \bar{b}\rho_0 - Z_0)}{\Gamma + 1} \rho_0 s^2. \quad (4.3.4)$$

In the present problem, the undisturbed density  $\rho_0$  is taken to vary according to the power law of the radius of the shock front  $R$  after the explosion and is given as

$$\rho_0 = \rho_a R^\alpha, \quad (4.3.5)$$

where  $\rho_a$  and  $\alpha$  are constants. The constant  $\alpha$  is to be determined later.

## 4.4 Exact solution of the blast wave problem

The R-H conditions (4.3.2)–(4.3.4) yields the following expression for the pressure behind the shock front

$$p = \frac{\Gamma - 1 + 2\bar{b}\rho_0 + 2Z_0}{2(1 - \bar{b}\rho_0 - Z_0)} \rho u^2. \quad (4.4.1)$$

By equation (4.3.5), equations (4.2.2) and (4.2.3), can be rewritten as

$$\frac{\partial u}{\partial t} + u \frac{\partial u}{\partial x} + K_1 \left( \frac{u^2}{\rho} \frac{\partial \rho}{\partial x} + 2u \frac{\partial u}{\partial x} \right) = 0, \quad (4.4.2)$$

$$\frac{\partial u}{\partial t} + u \frac{\partial u}{\partial x} + K_2 \left( \frac{\partial u}{\partial x} + \frac{m}{x} u \right) u = 0, \quad (4.4.3)$$

where  $K_1$  and  $K_2$  are given as

$$K_1 = \frac{\Gamma - 1 + 2\bar{b}\rho_0 + 2Z_0}{2(1 - \bar{b}\rho_0 - Z_0)},$$

$$K_2 = \frac{(\Gamma - 1 + 2\bar{b}\rho_0 + 2Z_0) [(\Gamma - 1)(\Gamma - 1 + 2\bar{b}\rho_0 + 2Z_0) + \alpha_1(\Gamma + 1)\rho_0] - 2\alpha_2(\Gamma + 1)^2 \rho_0^2}{2[(\Gamma - 1 + 2\bar{b}\rho_0 + 2Z_0) \{(\Gamma - 1 + 2\bar{b}\rho_0 + 2Z_0) - \alpha_1(\Gamma + 1)\rho_0\} + \alpha_2(\Gamma + 1)^2 \rho_0^2]}.$$

Combining (4.4.2) and (4.4.3) and after integration we have the resulting equation as,

$$f(t) = \rho u^\xi x^{-m\eta}, \quad (4.4.4)$$

where  $f(t)$  is function of time only and  $\xi$  and  $\eta$  are given as

$$\xi = (2K_1 - K_2) / K_1,$$

$$\eta = K_2 / K_1.$$

By equation (4.4.4) and (4.2.1), we have

$$\frac{\xi}{u} \frac{\partial u}{\partial t} - (1 - \xi) \frac{\partial u}{\partial x} - \frac{1}{f} \frac{df}{dt} - \frac{m(\eta + 1)}{x} u = 0. \quad (4.4.5)$$

Solving equations (4.4.3) and (4.4.5), we have

$$u = -\chi \frac{x}{f} \frac{df}{dt}, \quad (4.4.6)$$

where  $\chi$  is a constant given as

$$\chi = \frac{1}{(\xi K_2 + \eta + 1)m + (1 + \xi K_2)}, \quad (4.4.7)$$

also

$$f(t) = f_0 t^{-\tau}, \quad (4.4.8)$$

where  $f_0$  is arbitrary constant and  $\tau$  is given as

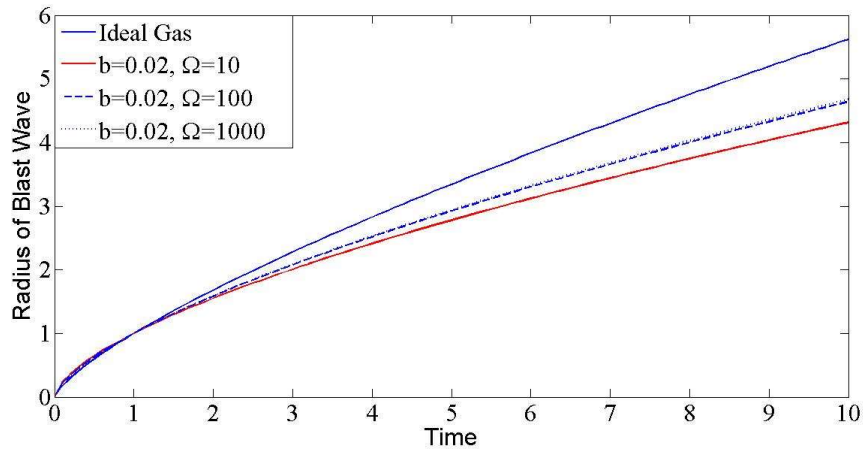
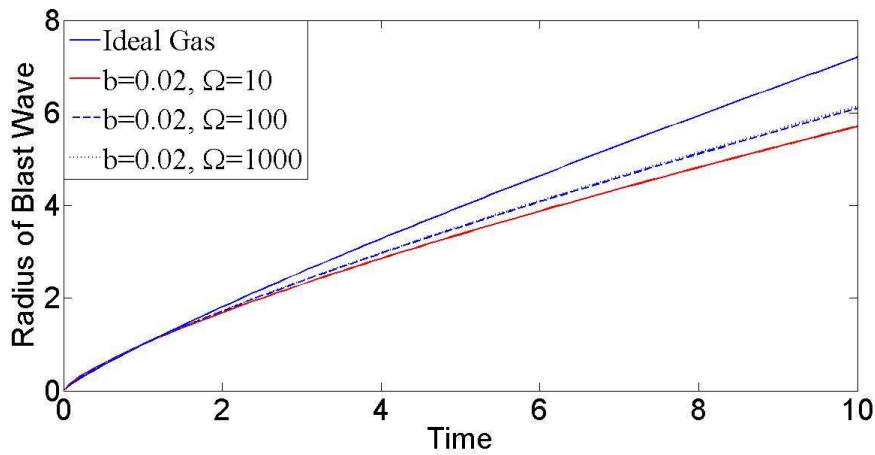
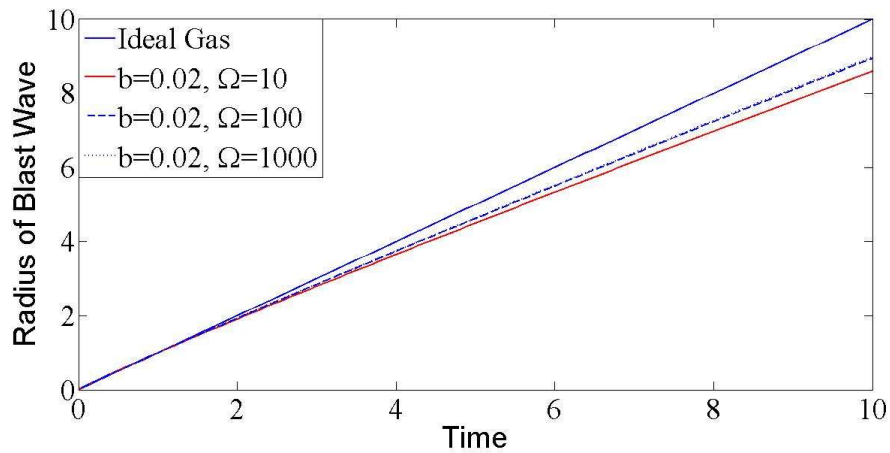
$$\tau = \frac{\xi}{(\xi - 1)\chi - m(\eta + 1)\chi + 1}.$$

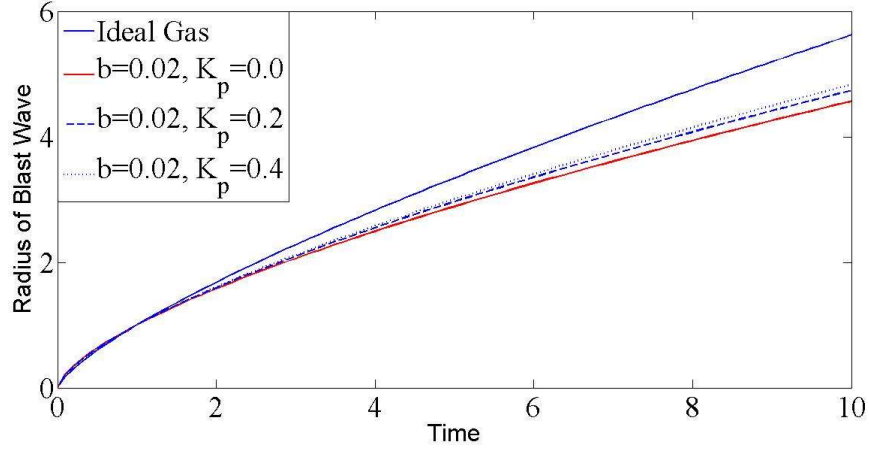
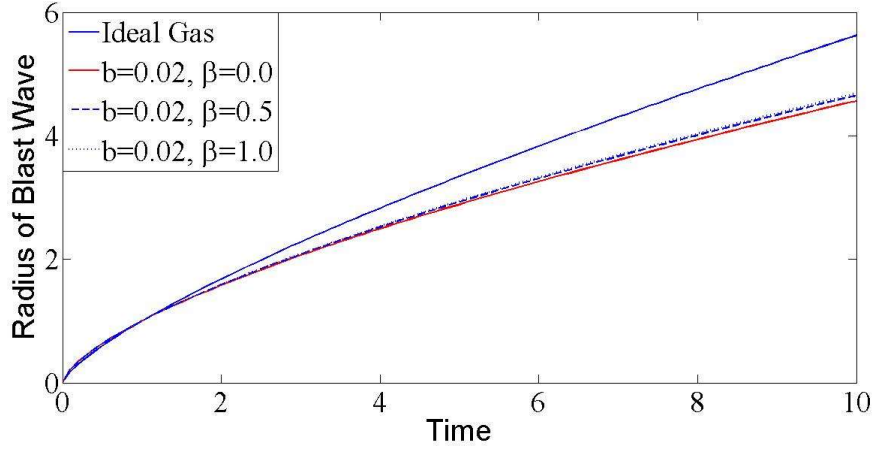
Rankine - Hugoniot condition (4.3.2) yields the analytical expression for the radius of the shock front as

$$R = t^{\frac{\Gamma+1}{(\Gamma-1+2b\rho_0+2Z_0)}\chi\tau}. \quad (4.4.9)$$

The effects of dust particles and non-idealness parameters on the radius of blast wave are shown in figures 4.1 - 4.5.

The effect of the density of the dust particles present in the gas on the radius of the blast wave in planar, cylindrically symmetric and spherically symmetric flows is shown in Figs. 4.1–4.3. The values of the constants appearing in the computations are taken as:  $\beta = 0.5$  and  $k_p = 0.1$ , and  $\Omega = 10, 100, 1000$ . It is observed that an increase in the density of dust particles in the mixture causes to increase the radius of blast wave whereas an increment in the non-idealness parameter causes to decrease the radius of the blast wave. From Fig.4.2 and Fig.4.3 it is clear that the variation of radius of the blast wave in cylindrically symmetric and planar flows have similar trend as in case of spherically symmetric flow but rate of variation is slowed down in planar case as compared to cylindrically symmetric and spherically symmetric flows. The rate of variation of radius in cylindrically symmetric flow is slowed down as compared to spherically symmetric flow. The effect of mass fraction and specific heat of the dust particles present in the gas on the radius of the blast wave at constants  $\Omega = 100$ ,  $\beta = 0.5$  and  $\Omega = 100$ ,  $k_p = 1.0$ , in spherically symmetric flows are shown in Figs. 4.4–4.5 respectively. Due to the similar behavior of solid particles in planar and cylindrically symmetric flows, details are omitted. Since increment in the mass fraction of solid particles have very less effect on the value of volume fraction of solid particles but have sufficient effect on the value of  $\Gamma$ . So, an increment in mass and specific heat of solid particles causes to increase the radius of the blast wave.

FIGURE 4.1: Behavior of the radius of the Blast Wave for  $m = 2$  with varying  $\Omega$ FIGURE 4.2: Behavior of the radius of the Blast Wave for  $m = 1$  with varying  $\Omega$ FIGURE 4.3: Behavior of the radius of the Blast Wave for  $m = 0$  with varying  $\Omega$

FIGURE 4.4: Behavior of the radius of the Blast Wave for  $m = 2$  with varying  $K_p$ FIGURE 4.5: Behavior of the radius of the Blast Wave for  $m = 2$  with varying  $\beta$ 

Rankine-Hugoniot condition (4.3.2) yields the following value of  $\alpha$  which is given as

$$\alpha = \frac{(n-1)(\Gamma+1) - 2(1 - \bar{b}\rho_0 - Z_0)\{(\eta+1)m - \xi + 1\}}{(\Gamma+1)}.$$

Therefore, the solution of strong shock wave problem is given as

$$\rho = \frac{f_0 t^{-\tau+\xi} x^{m\eta-\xi}}{\chi^\xi \tau^\xi}, \quad (4.4.10)$$

$$u = \chi^\tau \frac{x}{t}, \quad (4.4.11)$$

$$p = \frac{\Gamma - 1 + 2\bar{b}\rho_0 + 2Z_0}{2(1 - \bar{b}\rho_0 - Z_0)} \frac{1}{(\chi\tau)^{\xi-2}} f_0 x^{m\eta-\xi+2} t^{\xi-\tau-2}. \quad (4.4.12)$$

The effect of dust particles and non-ideal parameter on the spherically symmet-

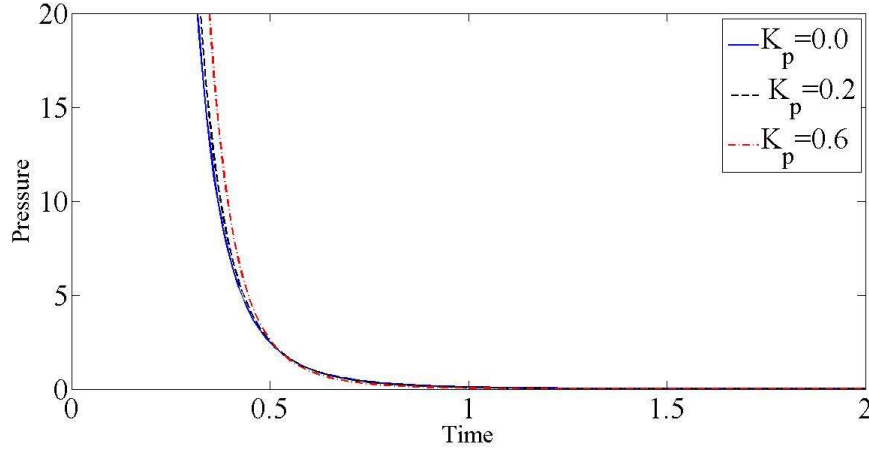


FIGURE 4.6: Pressure profiles for varying  $K_p$  with  $b = 0.02$ ,  $\beta = 0.5$  and  $\Omega = 100$ .

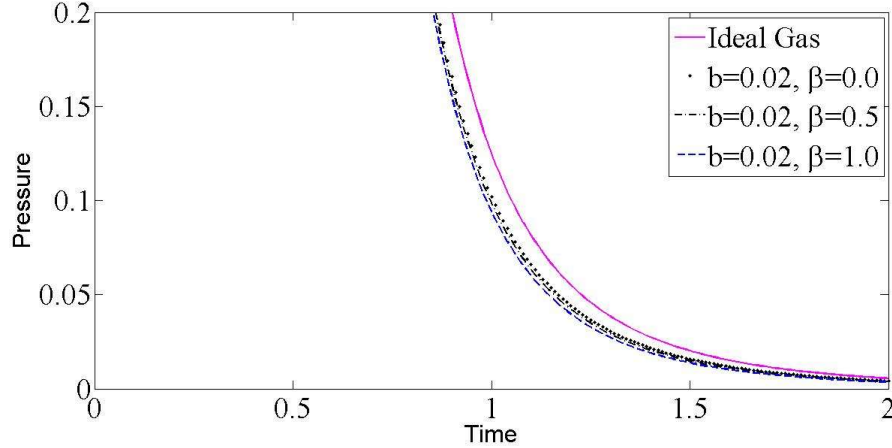


FIGURE 4.7: Pressure profiles for varying  $\beta$  with  $b = 0.02$ ,  $K_p = 0.1$  and  $\Omega = 100$ .

ric flow fields is shown in Figs. 4.6 - 4.19. Here it is observed that an increment in any one of the parameters among the mass concentration of dust particles, specific heat of solid particles and species density of solid particles results in an increment in the pressure, velocity and density of non-ideal dusty gas whereas the effect of an increment in the van der Waals excluded volume causes to decrease in the pressure,

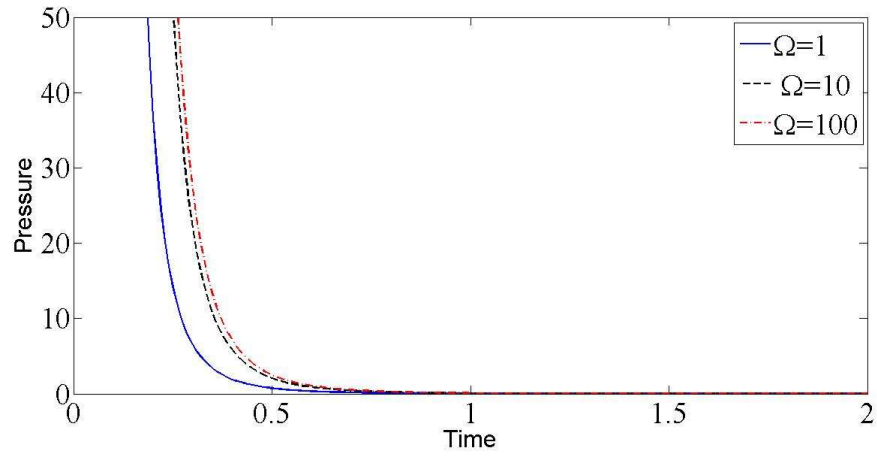


FIGURE 4.8: Pressure profiles for varying  $\Omega$  with  $b = 0.02$ ,  $K_p = 0.1$  and  $\beta = 0.5$ .

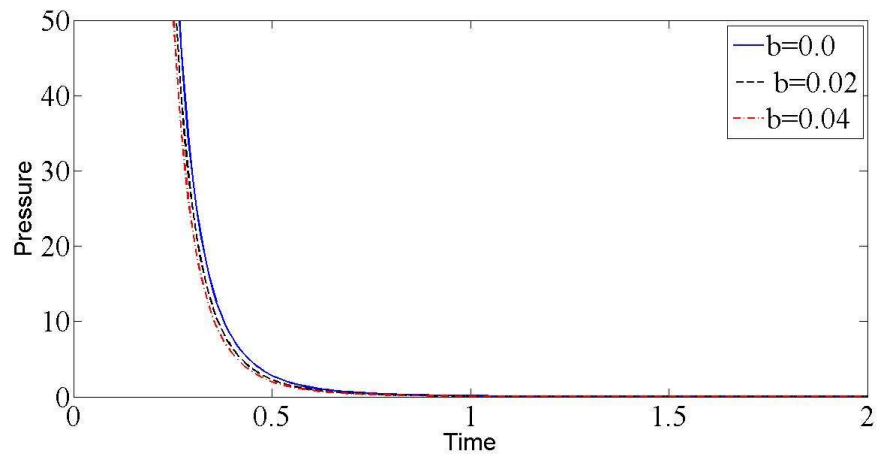


FIGURE 4.9: Pressure profiles for varying  $b$  with  $\Omega = 100$ ,  $K_p = 0.1$  and  $\beta = 0.5$ .

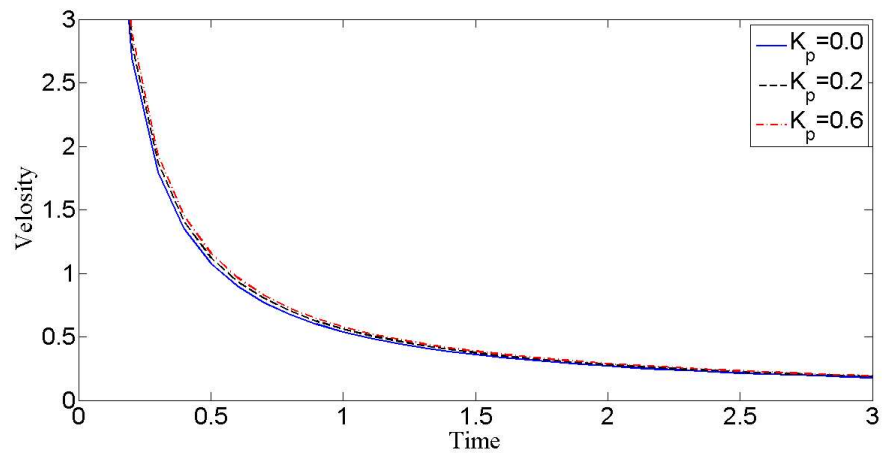
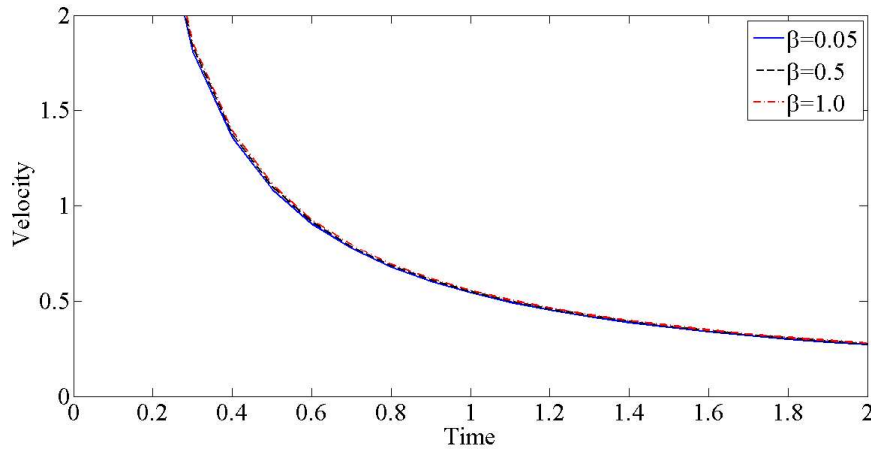
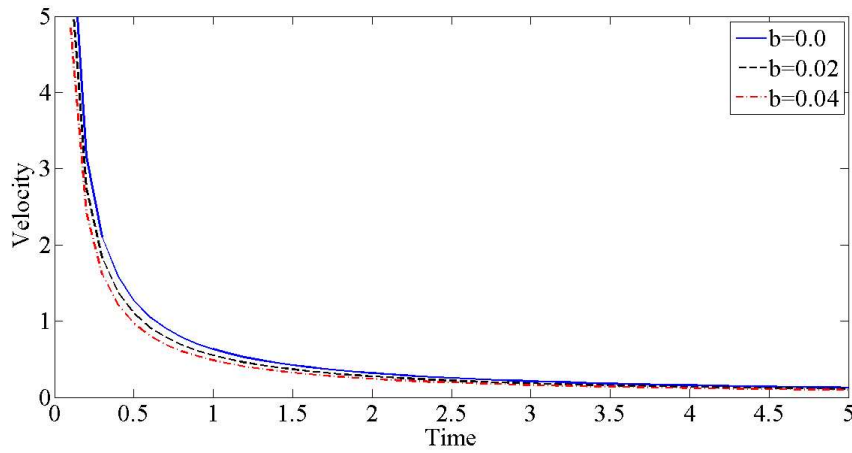
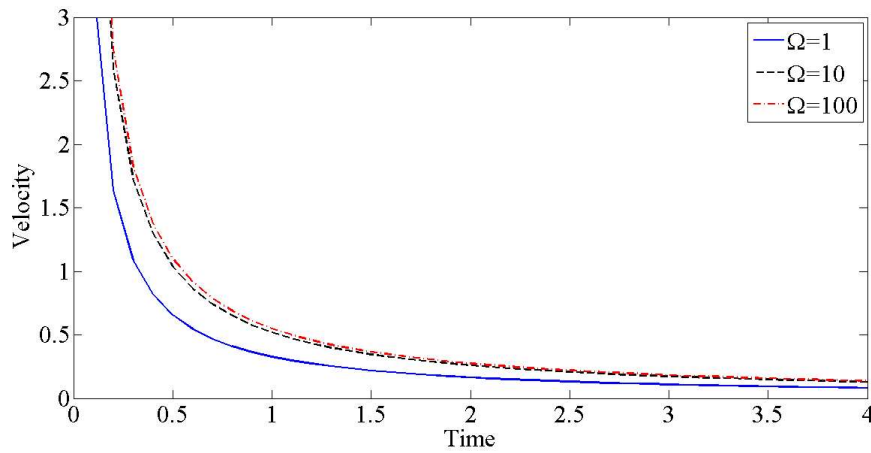


FIGURE 4.10: Velocity profiles for varying  $K_p$  with  $\Omega = 100$ ,  $b = 0.02$  and  $\beta = 0.5$ .

FIGURE 4.11: Velocity profiles for varying  $\beta$  with  $\Omega = 100$ ,  $K_p = 0.1$  and  $b = 0.02$ .FIGURE 4.12: Velocity profiles for varying  $b$  with  $\Omega = 100$ ,  $K_p = 0.1$  and  $\beta = 0.5$ .FIGURE 4.13: Velocity profiles for varying  $\Omega$  with  $b = 0.02$ ,  $K_p = 0.1$  and  $\beta = 0.5$ .

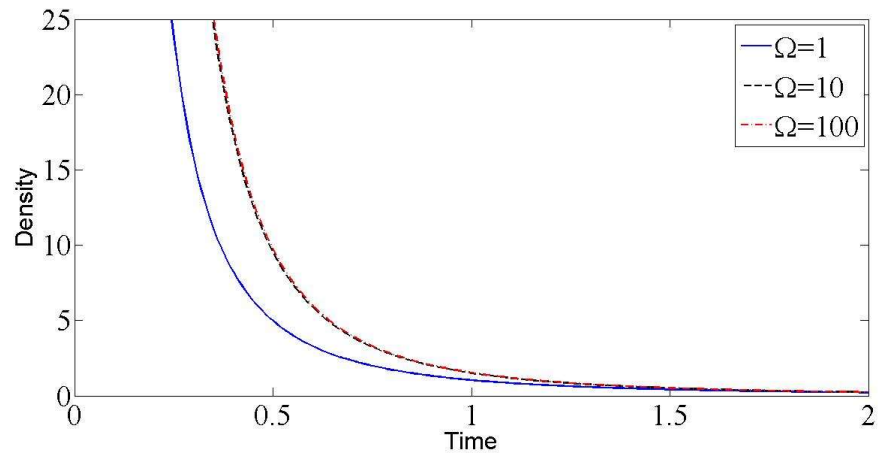


FIGURE 4.14: Density profiles for varying  $\Omega$  with  $b = 0.02$ ,  $K_p = 0.1$  and  $\beta = 0.5$ .

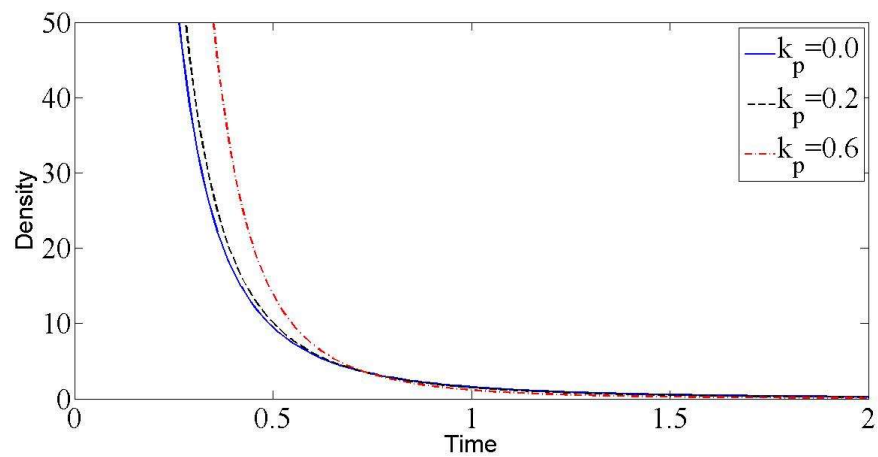


FIGURE 4.15: Density profiles for varying  $K_p$  with  $b = 0.02$ ,  $\Omega = 0.1$  and  $\beta = 0.5$ .

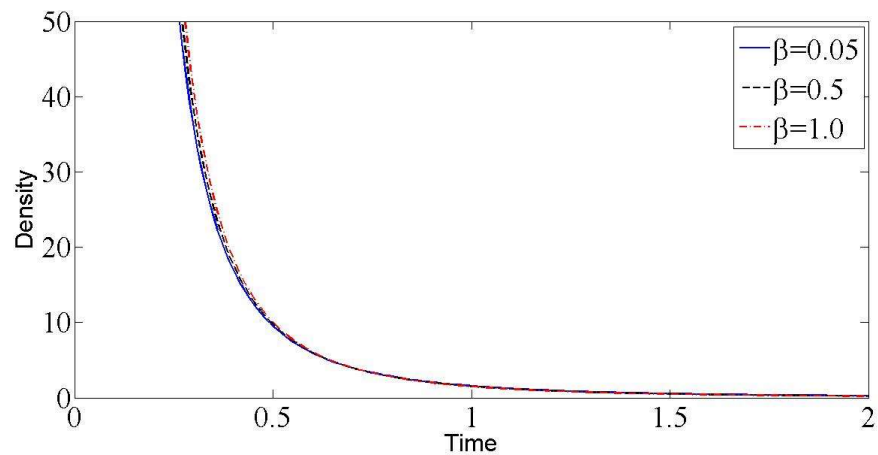


FIGURE 4.16: Density profiles for varying  $\beta$  with  $b = 0.02$ ,  $K_p = 0.1$  and  $\Omega = 100$ .

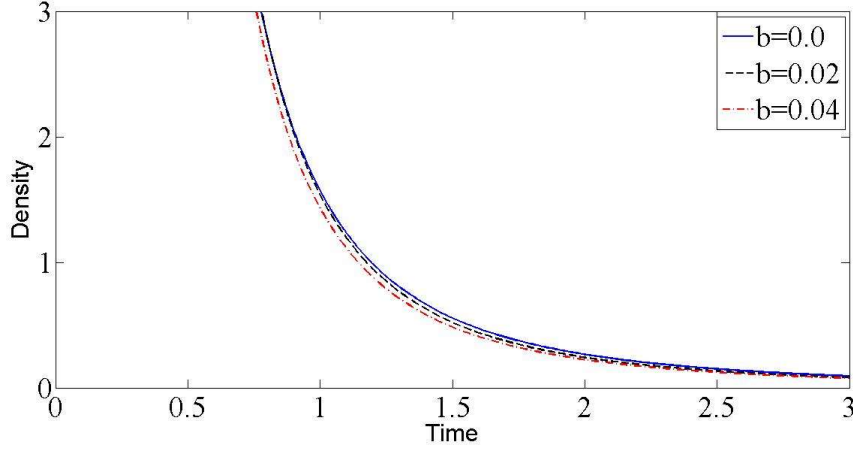


FIGURE 4.17: Density profiles for varying  $b$  with  $\Omega = 100$ ,  $K_p = 0.1$  and  $\beta = 0.5$ .

velocity and density of the non-ideal dusty gas.

After determining the physical quantities density, velocity and pressure behind the shock front, we can also calculate the total energy  $E$  (sum of kinetic and heat energy) within the blast wave in non-ideal dusty gas at any time  $t$  as Murata (2006)

$$\begin{aligned}
 E &= 4\pi \int_0^R \left\{ \frac{1}{2} \rho u^2 + \frac{(1-Z)(1-\bar{b}\rho)}{\Gamma-1} p \right\} x^m dx \\
 &= \frac{\left( \frac{1}{2} + \frac{(\Gamma-1+2Z_0+\bar{b}(3-\Gamma)\rho_0)(\Gamma-1+2Z_0+2\bar{b}\rho_0-Z_0(\Gamma+1)\rho_0)}{2(\Gamma-1)(1-Z_0\bar{b}\rho_0)(\Gamma-1+2Z_0+2\bar{b}\rho_0)} \right)}{3+m(\eta+1)-\xi} \\
 &\quad \times t^{2+\xi-\tau+\frac{(1+\Gamma)(3+m(\eta+1)-\xi)\chi\tau}{2(1-\bar{b}\rho_0-Z_0)}}
 \end{aligned}$$

The effects of density of the dust particles present in the gas and non-idealness parameter of gas on the energy carried by blast wave in spherically symmetric flows are shown in Fig.4.18. The values of the constants appearing in the computations are taken as:  $\beta = 0.5$ ,  $k_p = 0.1$ ,  $b = 0.02$  and  $\Omega = 10, 100, 1000$  and  $\rho_0 = 1$ . Here,

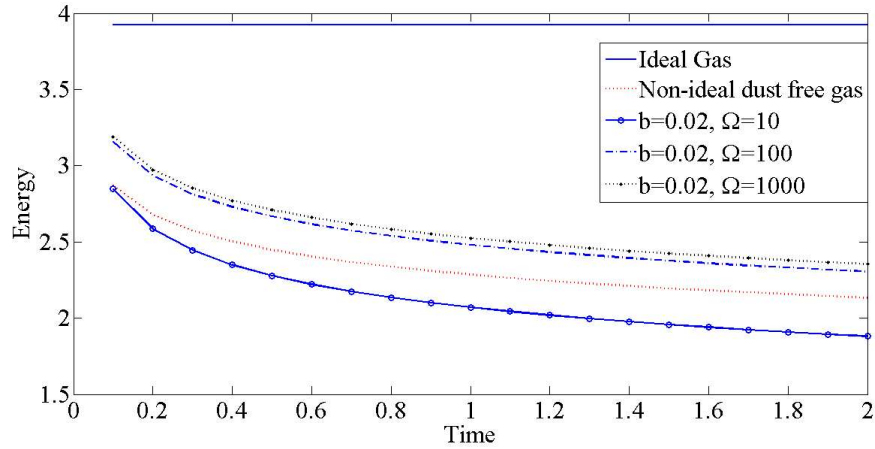


FIGURE 4.18: Behavior of energy carried by the blast wave for  $m = 2$  with varying  $\Omega$

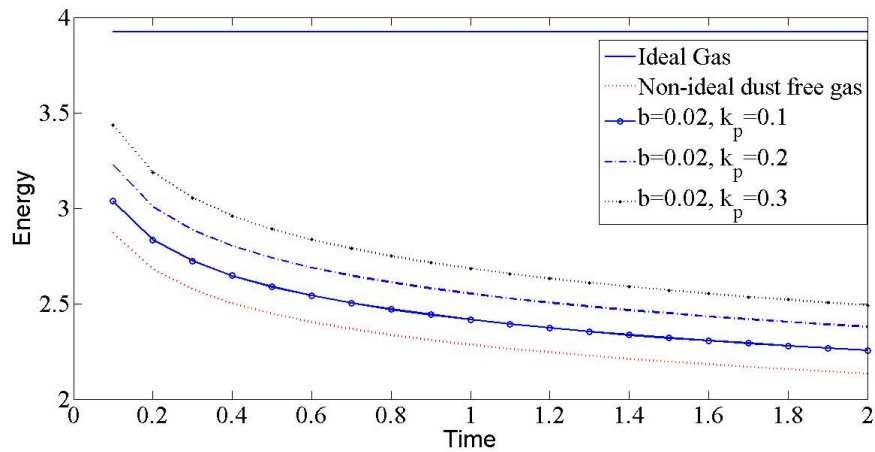


FIGURE 4.19: Behavior of energy carried by the blast wave for  $m = 2$  with varying  $K_p$

it is observed that the increment in the density of dust particles causes to increase the energy carried by blast wave in non-ideal gas whereas an increment in non-ideal parameter causes to decrease the energy carried by blast wave. The effects of mass fraction of the dust particles present in the gas on the energy carried by blast wave in spherically symmetric flows are shown in Fig.4.19. The values of the constants appearing in the computations are taken as:  $\beta = 0.5$ ,  $\Omega = 100$ ,  $b = 0.02$  and mass fraction  $k_p = 0.1, 0.2, 0.3$ . It is observed that an increment in the mass fraction of dust particles causes to increase the energy carried by blast wave in non-ideal

gas. Due to the similar effect of dust particles on the energy carried by blast wave, details are omitted. Here, it is observed that the solution of blast wave problem for adiabatic non-ideal dusty gas given by equation (4.4.10) –(4.4.12) reduces to the solution presented by Murata (2006) for  $\theta = b = 0$ .

## 4.5 Conclusion

In the present chapter, the exact analytical solution of the problem of blast wave in a non-ideal dusty gas for generalized geometries has been derived. The solution of Euler equation in a non-ideal dusty gas obtained here is a new one. The behavior of variations of the radius of blast wave in the mixture of non-ideal gas and small solid particles are similar to that as in an ideal and non-ideal gas where as the behavior of energy in a non-ideal dusty gas are quite different to that of an ideal gas and are similar to that of a non-ideal gas. Further, the solution of blast wave problem for adiabatic non-ideal dusty gas presented here reduces to the solution presented by some authors in past for ideal gas.

\*\*\*\*\*